



Article

Modeling Long-Distance Forward and Backward Diffusion Processes in Tracer Transport Using the Fractional Laplacian on Bounded Domains

Zhipeng Li ^{1,2,3} , Hongwu Tang ^{1,2,3,*}, Saiyu Yuan ^{1,2,3,*} , Huiming Zhang ¹, Lingzhong Kong ^{1,4} and HongGuang Sun ^{1,5}

- ¹ National Key Laboratory of Water Disaster Prevention, Hohai University, Nanjing 210098, China; zhipeng@hhu.edu.cn (Z.L.); hmzhang@hhu.edu.cn (H.Z.); 007396@yzu.edu.cn (L.K.); shg@hhu.edu.cn (H.S.)
² College of Water Conservancy and Hydropower Engineering, Hohai University, Nanjing 210098, China
³ Key Laboratory of Hydrologic-Cycle and Hydrodynamic-System of Ministry of Water Resources, Hohai University, Nanjing 210098, China
⁴ College of Hydraulic Science and Engineering, Yangzhou University, Yangzhou 225009, China
⁵ College of Mechanics and Materials, Hohai University, Nanjing 211100, China
* Correspondence: hwtang@hhu.edu.cn (H.T.); yuansaiyu@hhu.edu.cn (S.Y.)

Abstract: Recent studies have emphasized the importance of the long-distance diffusion model in characterizing tracer transport occurring within both subsurface and surface environments, particularly in heterogeneous systems. Long-distance diffusion, often referred to as nonlocal diffusion, signifies that tracer particles may experience a considerably long distance in either the forward or backward direction along preferential channels during the transport. The classical advection–diffusion (ADE) model has been widely used to describe tracer transport; however, they often fall short in capturing the intricacies of nonlocal diffusion processes. The fractional operator has gained recognition among hydrologists due to its potential to capture distinct mechanisms of transport and storage for tracer particles exhibiting nonlocal dynamics. However, the hypersingularity of the fractional Laplacian operator presents considerable difficulties in its numerical approximation in bounded domains. This study focuses on the development and application of the fractional Laplacian-based model to characterize nonlocal tracer transport behavior, specifically considering both forward and backward diffusion processes on bounded domains. The Riesz fractional Laplacian provides a mathematical framework for describing tracer diffusion processes on a bounded domain, and a novel finite difference method (FDM) is introduced as an effective numerical solver for addressing the fractional Laplacian-based model. Applications reveal that the fractional Laplacian-based model can effectively capture the observed nonlocal tracer transport behavior in a heterogeneous system, and nonlocal tracer transport exhibits dynamic characteristics, influenced by the evolving heterogeneity of the media at various temporal scales.

Keywords: fractional Laplacian; forward and backward diffusion; nonlocal model; heterogeneous systems; finite difference method



Citation: Li, Z.; Tang, H.; Yuan, S.; Zhang, H.; Kong, L.; Sun, H. Modeling Long-Distance Forward and Backward Diffusion Processes in Tracer Transport Using the Fractional Laplacian on Bounded Domains. *Fractal Fract.* **2023**, *7*, 823. <https://doi.org/10.3390/fractalfract7110823>

Academic Editors: Jordan Hristov, Sergei Fedotov, Boying Wu and Xiuying Li

Received: 26 September 2023
Revised: 7 November 2023
Accepted: 14 November 2023
Published: 15 November 2023



Copyright: © 2023 by the authors. Licensee MDPI, Basel, Switzerland. This article is an open access article distributed under the terms and conditions of the Creative Commons Attribution (CC BY) license (<https://creativecommons.org/licenses/by/4.0/>).

1. Introduction

The diffusion of tracer particles in natural systems, such as heterogeneous soils, aquifers, and rivers, is frequently characterized by non-Fickian behavior, often referred to as “anomalous” diffusion [1–4]. Anomalous diffusion is commonly encountered across various scales, ranging from soil core [5], laboratory experiments [6–8], to observations at the field-scale [9,10], among numerous others [11,12]. Anomalous diffusion, which encompasses subdiffusion (characterized by an MSD following a power-law relationship with time, i.e., $MSD(t) \propto t^\alpha$ with an exponent $\alpha < 1$) and superdiffusion (where $\alpha > 1$, which is often associated with active diffusion as investigated in the ten Hagen et al. [13], Ghosh et al. [14])

is a widespread phenomenon observed in a diverse array of both natural and engineered systems. These encompass a broad spectrum of domains, including porous media, as evidenced in Nelissen et al. [15], biological systems, as demonstrated in Taloni and Marchesoni [16], and turbulent fluid dynamics [17]. The emergence of anomalous diffusion typically arises due to the intricacies of nonuniform environments, the presence of obstacles, or the involvement of transport mechanisms that defy the conventional principles of Fickian diffusion [12,18]. Anomalous diffusion is significantly influenced by nonlocal transport processes occurring in spatial domains [18]. Nonlocal diffusion processes are an inherent characteristic of natural systems, primarily attributed to the occurrence of preferential flow paths [19]. Tracer particles demonstrate a proclivity to traverse preferred pathways in both forward and backward directions, ultimately resulting in the manifestation of non-Fickian behavior [18], as illustrated in the schematic diagram of nonlocal forward and backward diffusion processes depicted in Figure 1. The modeling of tracer nonlocal diffusion holds paramount significance as a research domain, offering profound implications for global-scale endeavors such as hydrocarbon exploration, groundwater resource management, hydraulic fracturing, and the secure disposal of high-level radioactive waste.

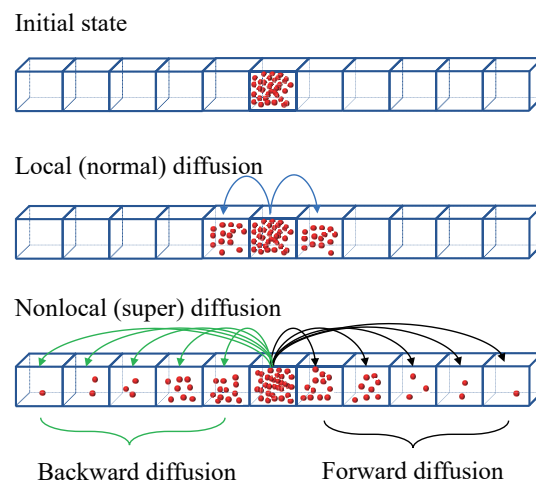


Figure 1. Conceptual map of the local and the nonlocal diffusion in both forward and backward directions.

Nonlocal diffusion denotes the characteristic in which the flux of tracer particles at a specific location is not solely determined by the gradient at that specific point, whether linear or nonlinear, but is instead an integrated flux that takes into account the heterogeneous characteristics of the surrounding environment [20,21]. The conventional depiction of passive tracer transport has traditionally relied upon a deterministic advection–diffusion equation (ADE) model, established through an analogy with Fick’s laws of diffusion [22]. Recently, a relatively novel stochastic framework centered on fractional-order derivatives has garnered growing interest among hydrologists [23–25]. This heightened attention is primarily due to the capacity of fractional-order derivative models to effectively capture alternative mechanisms of transportation and storage for tracer particles that exhibit non-Fickian transport dynamics [26]. In recent years, a considerable amount of research effort has been dedicated to the advancement of fractional advection–dispersion equation (FADE) theories, which are designed to comprehensively describe the intricate nature of anomalous tracer transport phenomena. This research has encompassed various aspects, including the incorporation of nonlocal boundary conditions into FADE models [27,28], the development of refined equation formulations that enhance our understanding of these transport processes [29,30], and the creation and refinement of both analytical and numerical methods for solving FADE [31]. Furthermore, it is worth noting that fractional calculus (FC) has emerged as a profound and interdisciplinary field within mathematics, with wide-ranging applications throughout various scientific and engineering disciplines.

Comprehensive insights into the manifold applications of FC can be found in the extensive discussion provided by Sun et al. [12].

Fractional models differ from the classical ADE model due to their ability to accommodate instances where tracer particles make substantial long-distance jumps [18]. This characteristic endows them with considerable utility in elucidating non-Fickian or nonlocal diffusion behavior that are commonly observed in a wide array of heterogeneous natural systems, including porous media, fractured networks, and turbulent flow environments [32,33]. Fractional operators, such as the fractional Laplacian [34], exhibit unique nonlocal properties, distinguishing them from their integer-order counterparts. These operators capture nonlocal effects by accounting for interactions between points in a system that extend beyond a fixed radius or distance, unlike classical differential operators that are local and rely on information from the immediate vicinity. The fractional Laplacian, for instance, characterizes the nonlocal behavior by considering the influence of distant points, allowing for the analysis of long-range dependencies or correlations within a system. These nonlocal properties play a significant role in various fields like physics, mathematics, and signal processing, offering a more nuanced understanding of phenomena that involve long-range interactions and complex behaviors.

In the realm of fractional models, researchers commonly employ a variety of definitions, including the Grünwald–Letnikov definition [35], the Riemann–Liouville definition [36], and several other alternatives [37], along with the fractional Laplacian. The fractional Laplacian operator, denoted as $(-\Delta)^{\alpha/2}$ with α belonging to the interval $(0, 2)$, possesses various equivalent characterizations [34]. However, the incorporation of boundary conditions necessitates distinct mathematical formulations in bounded domains [38,39]. Presently, there is no consensus within the scholarly literature regarding the most suitable definition of the fractional Laplacian in bounded domains for a given application. This study employs the Riesz fractional Laplacian, which introduces a specific nonlocal boundary condition, wherein the determination of a function's fractional Laplacian requires the specification of its values across the entire domain [34]. There are notable advantages associated with the direct utilization of the fractional Laplacian operator in characterizing the tracer diffusion process. Firstly, this operator provides a more transparent and physically interpretable framework compared to various definitions of fractional derivatives in characterizing the diffusion process [18]. Secondly, in contrast to one-sided definitions of fractional derivatives [37], the fractional Laplacian operator has the capability to concurrently account for both forward and backward diffusion processes experienced by tracer particles owing to its globally defined character. The above knowledge gaps inherent in classical fractional-derivative models motivated this study. This study aims to develop and employ a straightforward, physically grounded model for an in-depth examination of the stochastic aspects of nonlocal tracer transport dynamics, employing the fractional Laplacian operator, particularly on a bounded domain. A novel finite difference method is introduced for solving the fractional Laplacian-based model on a bounded domain, which offers a solution to a longstanding challenge in the field of nonlocal tracer transport modeling.

To reach the above goal, the rest of the paper is organized as follows. Section 2 of this paper presents a nonlocal advection–diffusion model based on the fractional Laplacian operator, and a novel finite difference method is introduced for its implementation. In Section 3, we delve into the diffusion regime of the model and conduct a sensitivity analysis of its parameters. Section 4 applies the fractional Laplacian model to simulate tracer transport scenarios documented in the existing literature. Conclusions are finally drawn in Section 5.

2. Materials and Methods

2.1. Model Development

In recent decades, researchers have extensively explored the domain of fractional calculus as a powerful tool for crafting sophisticated mathematical frameworks that can effectively describe complex anomalous systems [24]. The fractional Laplacian operator,

symbolized as $(-\Delta)^{\beta/2}$, stands out as a nonlocal extension of the classical Laplacian operator, finding relevance in a wide range of physical systems, including turbulent flows, porous media flows, pollutant transport, quantum mechanics, stochastic dynamics, and financial systems [12,19]. An emerging stochastic approach grounded in the framework of fractional derivatives has been increasingly drawing the interest of hydrologists [2,40]. This attention is due to its capacity to potentially capture unique mechanisms governing the transport and storage of tracer particles that display non-Fickian transport behavior. The fractional Laplacian is an integral operator defined over the domain \mathbb{R}^n . It is characterized by its definition as a pseudodifferential operator with the symbol $|k|^\beta$, as follows [41]:

$$(-\Delta)^{\beta/2} = \mathcal{F}^{-1} \left[|k|^\beta \mathcal{F}[u] \right], \quad \text{for } \beta > 0 \quad (1)$$

where \mathcal{F} represents the Fourier transform applied over the entire space \mathbb{R}^n , and it is accompanied by its inverse transform \mathcal{F}^{-1} . Notably, when $\beta = 2$, Equation (1) simplifies to the familiar spectral representation of the classical Laplace operator $(-\Delta)$.

The expression for the fractional Laplacian (1) is formulated in relation to the hypersingular integral, presented as follows [41]:

$$(-\Delta)^{\beta/2} u(x) = c_{n,\beta} P.V. \int_{\mathbb{R}^n} \frac{u(x) - u(y)}{|x - y|^{n+\beta}} dy, \quad \text{for } \beta \in (0, 2) \quad (2)$$

where the notation *P.V.* signifies the principal value integral, while the symbol $c_{n,\beta}$ represents a normalization constant, specifically defined as $\frac{2^{\beta-1} \beta \Gamma((\beta+n)/2)}{\sqrt{\pi^n} \Gamma(1-\beta/2)}$. Here, $\Gamma(x)$ denotes the Gamma function.

Equation (2) notably underscores that the evaluation of $(-\Delta)^{\beta/2} c$ at a given point $x \in \mathbb{R}^n$ is contingent upon the entire domain of values $c(y) : y \in \mathbb{R}^n$, given that the fractional Laplacian's definition encompasses the entire domain of \mathbb{R}^n . Nevertheless, in practical field applications, the nonlocal characteristics of tracer transport need to be constrained within bounded domains. It's important to note that, unlike the classical Laplacian operator, both the theoretical properties of the fractional Laplacian and its numerical handling are not yet comprehensively elucidated. Specifically, the inherent infinite nonlocal nature of the fractional Laplacian poses significant challenges when it comes to numerically approximating it within finite domains, especially in the context of characterizing tracer transport in heterogeneous media. The introduction of boundary conditions disrupts translational invariance, while the existence of long-range spatial correlations, inherent to the nonlocal properties of the fractional Laplacian operator, complicates the analysis of tracer transport [38]. One approach to define the fractional Laplacian on a bounded domain Ω is to apply the real space Formula (2) to functions on Ω , leading to the Riesz fractional Laplacian in Ω as follows [34]:

$$(-\Delta)^{\beta/2} u(x) = c_{n,\beta} \int_{\mathbb{R}^n} \frac{u(x) - u(y)}{|x - y|^{n+\beta}} dy = c_{n,\beta} \int_{\Omega} \frac{u(x) - u(y)}{|x - y|^{n+\beta}} dy + \int_{\mathbb{R}^n \setminus \Omega} \frac{u(x) - u(y)}{|x - y|^{n+\beta}} dy \quad (3)$$

This study investigates the fractional Laplacian on a one-dimensional bounded domain. Specifically, we delve into the discretization of the fractional Laplacian in the context of a one-dimensional bounded domain denoted as $\Omega = [0, L]$, where the domain size is represented by a constant value L . Consequently, the one-dimensional Riesz fractional Laplacian (3) can be reformulated as follows:

$$(-\Delta)^{\beta/2} c(x) = -c_{1,\beta} \left(\int_0^L \frac{c(x - \xi) - 2c(x) + c(x + \xi)}{\xi^{1+\beta}} d\xi + \int_L^\infty \frac{c(x - \xi) - 2c(x) + c(x + \xi)}{\xi^{1+\beta}} d\xi \right) \quad (4)$$

It is important to highlight that for any x within the interval $[0, L]$ and $\xi \geq L$, the function $c(x \pm \xi)$ is identically equal to zero in the context of tracer transport. Consequently, this leads to a simplification of the Riesz fractional Laplacian to the following expression:

$$\begin{aligned} (-\Delta)^{\beta/2}c(x) &= -c_{1,\beta} \left(\int_0^L \frac{c(x-\xi) - 2c(x) + c(x+\xi)}{\xi^{1+\beta}} d\xi + \int_L^\infty \frac{c(x-\xi) - 2c(x) + c(x+\xi)}{\xi^{1+\beta}} d\xi \right) \\ &= -c_{1,\beta} \left(\int_0^L \frac{c(x-\xi) - 2c(x) + c(x+\xi)}{\xi^{1+\beta}} d\xi - 2c(x) \int_L^\infty \frac{1}{\xi^{1+\beta}} d\xi \right) \\ &= -c_{1,\beta} \left(\int_0^L \frac{c(x-\xi) - 2c(x) + c(x+\xi)}{\xi^{1+\beta}} d\xi - \frac{2}{\beta L^\beta} c(x) \right) \end{aligned} \quad (5)$$

Finally, we incorporate the fractional Laplacian expression (5) into the classical retarded fractional advection–diffusion equation (F-ADE) model, resulting in the derivation of the following fractional model predicated on the fractional Laplacian operator (5):

$$R \frac{\partial c(x,t)}{\partial t} = -v \frac{\partial c(x,t)}{\partial x} - D \cdot (-\Delta)^{\beta/2} c(x,t), \quad x \in [0, L], \quad t > 0, \quad \beta \in (1, 2] \quad (6)$$

where R represents the retarded factor, v denotes the advection velocity of the tracer, and D stands for the diffusion coefficient.

Local tracer transport typically involves relatively straightforward particle movements that can be described based on the local conditions at a specific position x . In contrast, the fractional Laplacian-based model (6) pertains to nonlocal tracer transport, where particle motion spans sufficiently long distances forward or/and backward, as depicted in Figure 1. These nonlocal tracer transport processes encompass particle motions of significant scale, necessitating an understanding of how these movements relate to both upslope and downslope conditions, which may differ from the local conditions at the point x . A spatially nonlocal process arises when the concentration change at a specific location is not solely determined by the immediate surroundings but is also significantly impacted by the characteristics of a more extensive region in both the forward and backward directions from that point.

2.2. Finite Difference Method Scheme for the Fractional Laplacian-Based Model

As of now, there is a notable scarcity of numerical methods available for the discretization of the fractional Laplacian operator [42,43]. The primary numerical challenge in this context arises from the need to approximate the hypersingular integral accurately. In this study, a novel finite difference method (FDM) is presented to discretize the fractional Laplacian-based model (6) [41].

The above FDM introduces a splitting parameter denoted as $\gamma \in (\beta, 2]$, enabling the formulation of the fractional Laplacian (5) as the weighted integral of a weak singular function. Subsequently, this formulation is approximated using the weighted trapezoidal rule. Specifically, let us define a set of grid points as $x_i = i \cdot h$, where $0 \leq i \leq K$, and let \mathbf{c} be the vector represented as $(c(x_1, t), c(x_2, t), \dots, c(x_{K-1}, t))^T$. The numerical scheme can be formulated in matrix-vector notation, specifically as $(-\Delta)^{\beta/2} \mathbf{c} = \mathbf{A} \mathbf{c}$, where \mathbf{A} represents the matrix corresponding to the fractional Laplacian operator. The matrix \mathbf{A} is expressed as per the formulation in [41]:

$$A_{ij} = C_{\beta,\gamma}^h \begin{cases} \sum_{s=2}^{K-1} \frac{(s+1)^\nu - (s-1)^\nu}{s^\gamma} + \frac{K^\nu - (K-1)^\nu}{K^\gamma} + (2^\nu + \kappa_\gamma - 1) + \frac{2\nu}{\beta K^\beta}, & j = i, \\ -\frac{(|j-i|+1)^\nu - (|j-i|-1)^\nu}{2|j-i|^\gamma}, & j \neq i, i \pm 1, \\ -\frac{1}{2}(2^\nu + \kappa_\gamma - 1), & j = i \pm 1, \end{cases} \quad (7)$$

where for $i, j = 1, 2, \dots, K - 1$, we define $C_{\beta, \gamma}^h = c_{1, \beta} / (\nu h^\beta)$, and where $\nu = \gamma - \beta$, with $\kappa_\gamma = 1$ when γ lies in the interval $(0, 2)$ and $\kappa_\gamma = 2$ if $\gamma = 2$. Additionally, γ is constrained to the range $(\beta, 2]$. Duo et al. [41] proved that various selections of γ yield identical convergence rates, while the numerical errors are usually smaller when choosing $\gamma = 1 + \beta/2$. Hence, we employ $\gamma = 1 + \beta/2$ in the subsequent numerical calculations. As demonstrated by Duo et al. [41], for sufficiently smooth functions, the accuracy of the aforementioned FDM for the fractional Laplacian can be elevated to $o(h^2)$ uniformly across the entire range of $\beta \in (0, 2)$.

As the parameter β approaches 2, the scheme with $\gamma = 2$ effectively transforms into the central difference scheme for the classical Laplacian operator as follows:

$$-\Delta_h c_i = \frac{1}{h^2} (-c_{i-1} + 2c_i - c_{i+1}) \quad (8)$$

Additionally, we approximate the first-order time and spatial derivatives of model (6) using the equations below:

$$\frac{\partial c(x, t)}{\partial t} = \frac{c_i^{k+1} - c_i^k}{\Delta t} + o(\Delta t), \quad \frac{\partial c(x, t)}{\partial x} = \frac{c_{i+1}^{k+1} - c_i^{k+1}}{h} + o(h) \quad (9)$$

By defining $v_i = v/R$ and $D_i = D/R$, we establish the matrix denoted as B in the following manner:

$$B_{ij} = \begin{cases} 1 - \frac{v_i \Delta t}{h}, & j = i, \\ \frac{v_i \Delta t}{h}, & i = j - 1, \\ 0, & i \neq j, j - 1. \end{cases} \quad (10)$$

Hence, the equations corresponding to the fractional Laplacian-based model (6) can be formulated by taking into account an implicit scheme as follows:

$$\mathbf{M}\mathbf{c}^{k+1} = \mathbf{c}^k \quad (11)$$

where $\mathbf{M} = D_i \Delta t \cdot \mathbf{A} + \mathbf{B}$.

Finally, the following numerical solution is obtained:

$$\mathbf{c}^{k+1} = \mathbf{M}^{-1} \mathbf{c}^k \quad (12)$$

Figure 2 illustrates the temporal evolution of $c(x, t)$ with an instantaneous initial condition $c(x, 0) = \delta(x)$ and with a Neumann boundary condition $\frac{\partial c(x, t)}{\partial x} \Big|_{x=L} = 0$. The concentration profiles are computed using the aforementioned implicit FDM scheme. The results demonstrate that this implicit FDM approach provides a stable solution for the fractional Laplacian-based model (6). Notably, the snapshots in Figure 2a display significant skewness characteristics. This phenomenon can be attributed to the consideration of a bounded domain ($x \in [0, 500]$ m) and the inherent asymmetry in nonlocal regions between upstream and downstream points. Additionally, Figure 2b indicates that the snapshots at all time steps exhibit early-arrival behavior. The early arrivals are influenced by spatial nonlocal transport processes, which are of paramount significance in terms of potential risks.

It is noteworthy that our presented FDM is primarily designed for 1D problems due to their relative computational tractability. Addressing the hypersingularity associated with the fractional Laplacian operator in higher dimensions indeed presents a significant numerical challenge. Future research should encompass a thorough investigation into numerical algorithms tailored for addressing the challenges posed by high-dimensional fractional Laplacian problems.

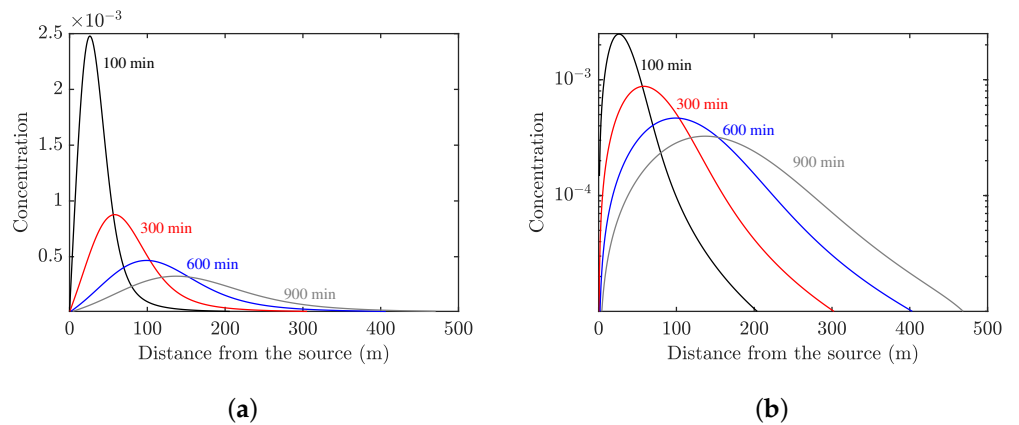


Figure 2. Simulated tracer concentration of the fractional Laplacian-based model (6) using the implicit FDM scheme. (a) The snapshots of the fractional Laplacian-based model at different times. (b) The semilog plot of snapshots at different times. All parameters are set as $\beta = 1.4$, $v = 0.1$ m/min, $D = 0.4$ m $^\beta$ /min, $R = 1$, and $\gamma = 1.7$.

3. Results and Discussion

3.1. Diffusion Regimes

An established method for investigating the stochastic movement of Brownian tracers involves assessing the mean squared displacement (MSD) of these tracer particles. In a manner analogous to Brownian motion, this subsection is dedicated to the evaluation of the fractional Laplacian-based model by employing MSD as a metric for quantifying nonlocal tracer transport behavior. The MSD is defined as follows [44]:

$$R_{MSD}(t) \propto A \cdot t^\eta \tag{13}$$

The MSD provides insight into the extent to which tracer particles deviate from their mean position. Equation (13) provides a pivotal insight into classifying the diffusion characteristics of nonlocal tracer transport, primarily contingent on the value of the exponent η . Specifically, when $\eta > 1$, it signifies superdiffusion; when $\eta < 1$, it signifies subdiffusion; and when $\eta = 1$, it corresponds to normal diffusion (Brownian motion) [24]. This classification underscores the significance of the exponent η in discerning different diffusion regimes within nonlocal tracer transport.

Here, let $\mu(x) = \frac{c_{1,\beta}}{|x|^{1+\beta}}$, and the fractional Laplacian-based model (6) can be rewritten as:

$$\begin{aligned} \frac{\partial c(x,t)}{\partial t} &= -v_i \frac{\partial c(x,t)}{\partial x} - D_i \cdot \int_{\mathbb{R}} \mu(x-x')c(x,t)dx' + D_i \cdot \int_{\mathbb{R}} \mu(x-x')c(x',t)dx' \\ &= -v_i \frac{\partial c(x,t)}{\partial x} + D_i \cdot [\mu * c](x,t) - D_i \cdot \beta_1 \cdot c(x,t) \end{aligned} \tag{14}$$

where $(*)$ denotes the convolution operator $[\mu * c](x,t) = \int_{\mathbb{R}} \mu(x-x')c(x,t)dx'$, and $\beta_1 = \int_{\mathbb{R}} \mu(x)dx$.

Taking the Fourier transform of Equation (14), one obtains:

$$\frac{\partial \hat{c}(k,t)}{\partial t} = (-v_i k i + D_i \cdot \hat{\mu}(k) - D_i \cdot \beta_1) \hat{c}(k,t) \tag{15}$$

Taking into account the initial point source condition $c(x,0) = \delta(x)$, which leads to $\hat{c}(k,0) = 1$, the solution to Equation (15) in the Fourier space can be expressed as follows:

$$\hat{c}(k,t) = \exp([-v_i k i + D_i \cdot \hat{\mu}(k) - D_i \cdot \beta_1]t) \tag{16}$$

To perform the Fourier transform of $\mu(x)$, we employ a specific technique involving the integral $\int_{\mathbb{R}} \mu(x) dx = 1$ to facilitate the process:

$$\begin{aligned}\hat{\mu}(k) &= 1 - (1 - \hat{\mu}(k)) = 1 - \int_{\mathbb{R}} (1 - \cos kx) \mu(x) dx \\ &= 1 - \frac{1}{k} \int_{\mathbb{R}} (1 - \cos y) \mu\left(\frac{y}{k}\right) dy \cong 1 - \frac{1}{k} \int_{\mathbb{R}} (1 - \cos y) \frac{c_{1,\beta}}{|y/k|^{1+\beta}} dy \\ &= 1 - c_{1,\beta} |k|^\beta \int_{\mathbb{R}} \frac{(1 - \cos y)}{|y|^{1+\beta}} dy = 1 - A |k|^\beta\end{aligned}\quad (17)$$

The integral in the final line of Equation (17) exhibits convergence when $\beta < 2$, and Equation (17) can be expressed as follows:

$$\hat{\mu}(k) = 1 - \frac{c_{1,\beta} \cdot \pi}{\Gamma(1 + \beta) \sin(\pi\beta/2)} |k|^\beta \quad (18)$$

with

$$\beta_1 = \int_{\mathbb{R}} \mu(x) dx = \hat{\mu}(0) = 1 \quad (19)$$

Finally, the solution of (16) can be expressed as:

$$c(x, t) = \mathcal{F}^{-1} \left[\exp \left(-v_i k i - D_i \cdot \frac{c_{1,\beta} \cdot \pi}{\Gamma(1 + \beta) \sin(\pi\beta/2)} |k|^\beta \right) t \right] \quad (20)$$

where \mathcal{F}^{-1} represents the inverse Fourier transform.

The MSD can be calculated for the solution given by Equation (20) in the case of $v = 0$. The analytical solution for $c(x, t)$ can be obtained by employing Fox functions, yielding the following result [18]:

$$c(x, t) = \frac{1}{\beta |x|} H_{2,2}^{1,2} \left[\frac{|x|}{(K_\beta t)^{1/\beta}} \middle| \begin{matrix} (1,1/\mu), (1,1/2) \\ (1,1), (1,1/2) \end{matrix} \right] \quad (21)$$

Equation (21) serves as a closed-form representation of a Lévy stable law. As $\beta = 2$, the classical Gaussian solution is regained, as dictated by established theorems concerning Fox functions. In the case of $\beta < 2$, the MSD of the fractional Laplacian-based model diverges:

$$R_{MSD}(t) \rightarrow \infty \quad (22)$$

Here, a fractional moment is introduced as a means to quantify the MSD of the fractional Laplacian-based model described by Equation (6). The generalized MSD can be expressed as follows [18]:

$$R_{MSD}(t) \propto \tilde{K} \cdot t^{2/\beta} \quad (23)$$

Equation (23) provides insight into the behavior of the fractional Laplacian-based model (6). It indicates that the model exhibits superdiffusion characteristics when $\beta < 2$, while normal diffusion behavior is observed when $\beta = 2$.

3.2. Sensitivity Analysis of Model Parameters

Fractional order β stands as the sole parameter governing the superdiffusion characteristics of tracer particles in the fractional Laplacian-based model presented in Equation (6).

Superdiffusion within tracer transport introduces two notable characteristics to the breakthrough curves (BTCs) and snapshots of tracer particles. Firstly, in the BTCs, there is an early-arrival pattern, indicating the rapid advancement of tracer particles through the medium. Secondly, heavy-tailed distributions are observed in the snapshots, signifying the propensity of tracer particles to undergo long-distance displacements. Here, we investigate the snapshots and BTCs of the model with a different fractional order β using the above-mentioned FDM.

Figure 3 presents numerical results for the fractional Laplacian-based model described in Equation (6) under varying fractional orders β with an instantaneous source. The comparisons include snapshots and BTCs with four distinct sets of parameters for instantaneous sources. The simulation outcomes reveal that, as β decreases, the snapshots exhibit increased dispersion, as presented in Figure 3a. Additionally, the tails of the snapshots become heavier for smaller values of β . This feature is attributed to the fact that smaller β values correspond to stronger nonlocal interactions within bounded domains for tracer transport. Moreover, the occurrence of early arrivals in tracer concentration profiles becomes more pronounced as the fractional order parameter β decreases, as shown in Figure 3b. Early arrival refers to the detection of a tracer concentration at an earlier time interval at a specific location. This phenomenon can be articulated as follows: “When conducting sampling activities in heterogeneous soils or aquifers, tracer particles may encounter various velocity zones. In the presence of a complex heterogeneity structure, such as spatial connectivity, particle movement within a certain scale can be facilitated. Under such conditions, rapid movements may deviate from classical Fick’s law and exhibit a probability density function that follows a power-law distribution.” The superdiffusion behavior described by the model (Equation (6)) represents one manifestation of such long-distance movements. The results obtained from the snapshots and BTCs indicate that, as the value of β approaches 2, the simulated snapshots and BTCs exhibit a notable trend towards symmetry, resembling a Gaussian plume, as illustrated in Figure 3a,b. Additionally, it is important to emphasize that, with the approach of β to 2, the nonlocal effects diminish, resulting in tracer transport behavior predominantly influenced by local conditions.

The early-arrival and heavy-tailed features hold substantial significance in practical applications. For instance, in groundwater management, an accurate understanding of the transport behavior of pollutants or solutes is crucial as it directly impacts the quality and sustainable utilization of water resources. Additionally, comprehending these superdiffusion characteristics is of paramount importance in fields such as hydrocarbon exploration and development in geological reservoirs and the migration and disposal of hazardous substances in environmental engineering processes.

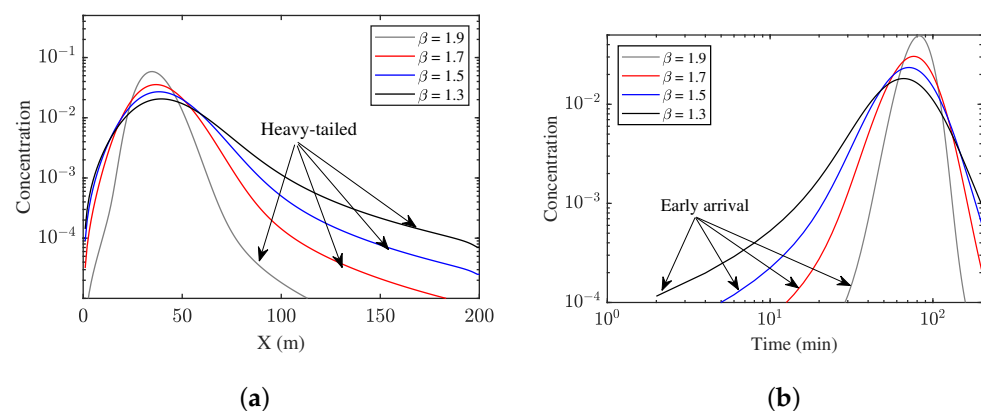


Figure 3. The snapshots and BTCs with different values of fractional order β for the fractional Laplacian-based model (6). The fractional order β varies from 1.3 to 1.9. (a) The spatial distribution of tracer particles at $T = 60$ min. (b) The temporal evolution of tracer particles at $X = 100$ m. Other parameters are set as $v = 0.6$ m/min, $D = 0.4$ m ^{β} /min, $R = 1$, and $\gamma = 1 + \beta/2$.

4. Applications

4.1. Case 1: Solute Transport in Groundwater Flow

In this section, we assess the suitability of the fractional Laplacian-based model (6) for quantifying nonlocal tracer transport as reported in the literature by Yin et al. [45]. Yin et al. [45] conducted a comprehensive study on tracer particle dynamics in an alluvial setting characterized by heterogeneity. They created a two-dimensional representation of various alluvial settings with diverse hydrofacies structures using the T-PROGS method and simulated conservative tracer transport using the Monte Carlo approach. These structures represent realistic heterogeneous conditions commonly encountered in natural aquifers and subsurface environments. Such realism is crucial for evaluating the model's performance in practical, complex systems. The dataset includes snapshots of tracer concentrations at different time intervals (e.g., 27 days, 132 days, 224 days, and 328 days). This temporal evolution is vital because it allows for the observation of changes in the tracer distribution over time. The model must be capable of capturing how nonlocal transport behavior evolves as time progresses, making this dataset ideal for such an analysis, and the detailed information regarding this study can be found in their publication [45].

The experimental data clearly show observable changes in the trailing edge of the tracer plume as time advances, and the feature suggests an increasing influence of nonlocal transport behavior over time. These empirical findings serve as a valuable dataset that enable us to examine and validate the applicability of the fractional Laplacian-based model (6) in describing nonlocal tracer transport dynamics in heterogeneous media. By comparing the model's predictions to the observed changes in the tracer distribution over time, we can assess how well the model captures the evolving nonlocal behavior in such systems. In our analysis, we utilized the first snapshot of the dataset, specifically the data collected at 27 days, to estimate the parameters v , D , and R for the fractional Laplacian-based model. Subsequently, we employed these estimated parameters to predict the behavior observed in later snapshots, adjusting the fractional order β as needed. For the sake of comparison, we also calculated results using the classical ADE model.

Figure 4a–d depict the fitting results obtained from the fractional model for each snapshot. These results illustrate that the fractional Laplacian-based model adeptly captures the intricate nonlocal transport behavior observed in the dataset. Conversely, the ADE model falls short in reproducing the observed behavior, highlighting its limitations in representing such complex phenomena. Table 1 lists the best-fitting parameters of the fractional-Laplacian model. Notably, the results reveal a decreasing trend in the fractional order parameter β as time progresses, a trend that closely aligns with the dataset. This diminishing value of β over time corresponds to an intensified superdiffusion behavior, indicating that space nonlocal transport processes exhibit dynamic behavior that evolves across various time scales.

Table 1. The best-fit parameters for the fractional Laplacian model.

Time (Days)	v (m/day)	D (m ^{β} /day)	R	β
27				1.40
132	0.018	3	10	1.30
224				1.25
328				1.16

Moreover, Figure 5a provides a temporal evolution of the best-fit β values, revealing a linear correlation between the fractional order parameter β and time. Figure 5b illustrates the progressive enhancement of superdiffusion behavior over time. Specifically, following the initial day, the superdiffusion rate significantly surpasses that of normal diffusion. After the 40th day, a more conspicuous acceleration in the growth of the mean squared displacement is observed, further accentuating the influence of superdiffusion.

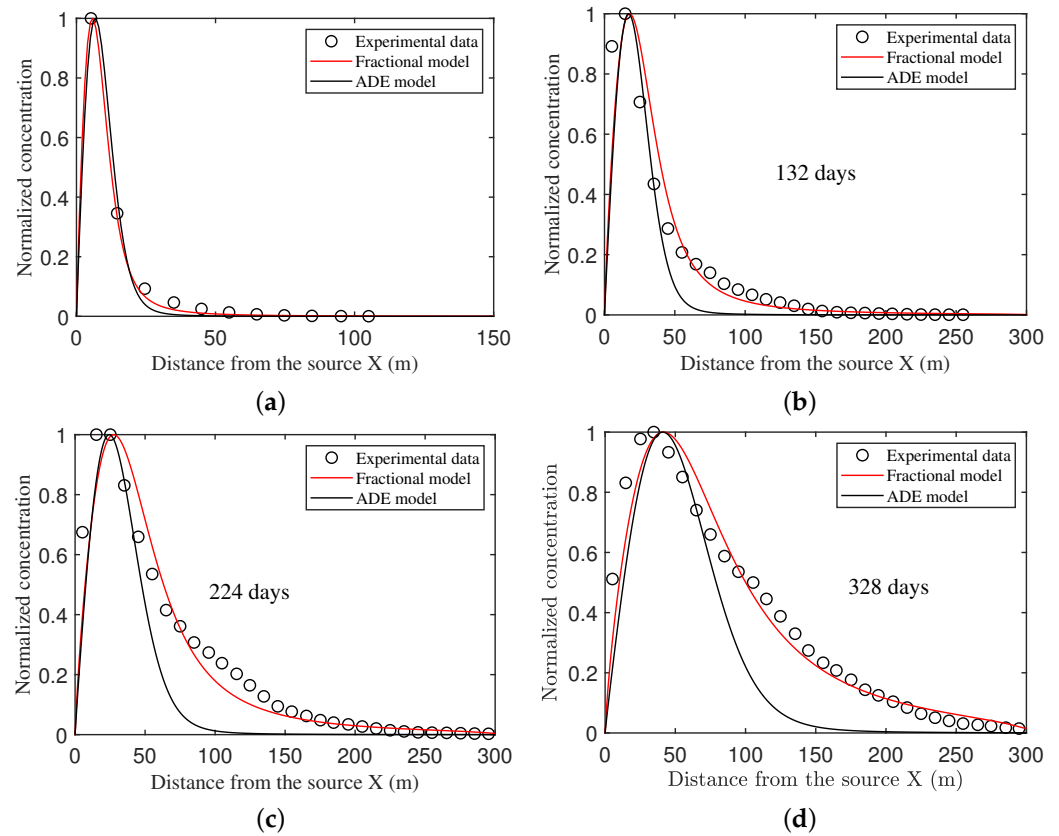


Figure 4. Comparison between the documented snapshots (symbols) and the best-fit results using the classical ADE and fractional Laplacian-based models at four times ($t = 27, 132, 224,$ and 328 days) along the 300 m long heterogeneous media. All parameters are list in Table 1. (a) 27 days, (b) 132 days, (c) 224 days, and (d) 328 days.

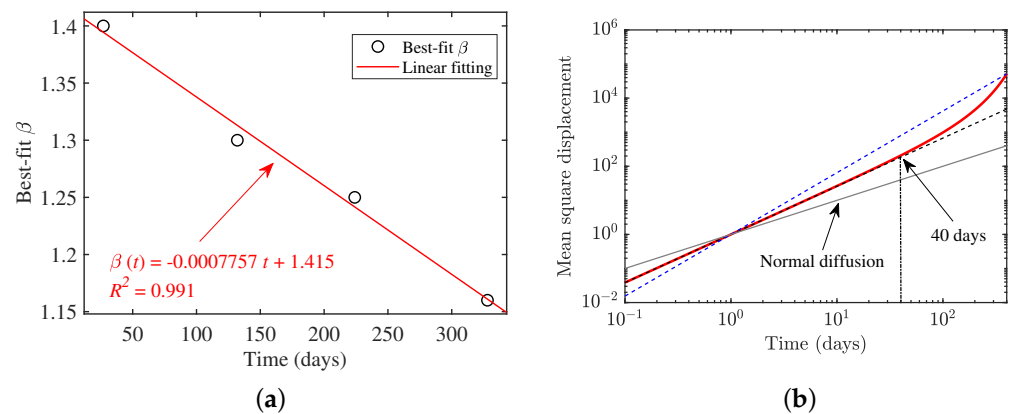


Figure 5. (a) The fitting results for the fractional order β and its variation with time. (b) The evolution of the tracer particle mean squared displacement (MSD) with time (red solid line), and the MSD for normal diffusion (gray solid line) is included for comparison. The gray and blue dashed lines represent the evolution trend of MSD at early and later times, respectively.

In summary, the application underscores the effectiveness of the fractional Laplacian-based model, with its variable fractional order β , in capturing the evolving nonlocal transport behavior evident in the dataset. Conversely, the classical ADE model proves inadequate in replicating the intricacies of the observed tracer transport dynamics in heterogeneous media. These findings emphasize the utility of the fractional Laplacian-based model in characterizing nonlocal behavior within real-world, heterogeneous subsurface systems. Moreover, the changing nature of the fractional order parameter β with time high-

lights the dynamicity of space nonlocal transport processes and their sensitivity to temporal scales. The variation in diffusion rates at different time intervals further underscores the significant impact of media heterogeneity on tracer transport dynamics.

4.2. Case 2: Intermediate-Scale Flume Experiments of Bedload Sediments

Laboratory experiments were conducted within a flume measuring 20 m in length, 1 m in width, and 1.2 m in depth. The flume was filled with sediment of varying diameters, which included 0.45 mm, 1 mm, 3 mm, and 17 mm, as detailed in the grain size distribution (GSD) information provided in Li et al. [4]. This flume experiment was deliberately designed to provide data at an intermediate scale, bridging the gap between 2D flume experiments and real river systems. The dimensions of the flume are approximately one order of magnitude larger than those of the 2D flume, facilitating a 3D evolution of the channel bed. Flume experiments were undertaken to investigate the dynamics of bedload transport under conditions characterized by low Shields stress. The initial slope of the channel bed was set at 0.004. To ensure a uniform sediment input across the channel width, a bedload feeder was positioned at the upstream section of the flume. The inflow discharge, quantified using an electromagnetic flow meter, ranged from 120 L/s to 140 L/s. The Froude number consistently remained below 1, with values ranging from 0.63 to 0.65, indicating that the flow within the flume was subcritical in nature.

The experimental findings offer compelling evidence for the presence of nonlocal bedload transport phenomena. Within the mixed-size gravel beds, a notable phenomenon emerges as larger particles tend to congregate into clusters as they lack individual resistance against hydraulic forces. This clustering effect results in the development of microrelief features within the armor layer, including the formation of these clusters and the occurrence of what can be termed as “flow accelerating belts” between them [4]. Sediment particles that were previously trapped within disintegrated clusters may undergo sudden release and travel significant distances along these “flow accelerating belts” until they are once again captured by other clusters. This intricate process gives rise to nonlocal bedload transport behavior, wherein the movement of sediment is not confined to localized areas [4]. Consequently, the flume experiments furnished valuable data for the purpose of model validation.

Figure 6 presents the best-fitting results of three different models: the classical ADE model (black lines), the PD model (blue lines) [4], and the fractional Laplacian-based model (red lines). The parameters for each model were determined by fitting the initial snapshot taken at 155 min and subsequently predicting the behavior at a later time point, specifically 355 min. The fitting results shed light on the limitations of the local model, as it fails to capture the nonlocal characteristics (heavy-tailed) observed in the bedload sediment snapshots. In contrast, both the PD model and the fractional Laplacian-based model exhibit the ability to replicate the heavy-tailed nature of the snapshots. A detailed analysis of two snapshots reveals that the fractional Laplacian-based model effectively captures the trends observed from the early to later time, particularly in the upstream region. It is important to note that the PD model tends to overestimate the upstream sediment concentration in the early-time scenario while underestimating it at later times. Additionally, unlike the PD model, which involves the determination of influence domain and influence functions in simulations, the fractional Laplacian-based model features only one additional parameter (the order of the fractional derivative). This simplicity in parameter determination renders the fractional Laplacian-based model more practical and user-friendly in applications.

The applications mentioned above demonstrate that the fractional Laplacian-based model effectively captures nonlocal tracer transport behavior, providing enhanced insights into the presence of early-arrival and heavy-tailed features within these tracer transport systems. For instance, in the context of groundwater management, our model offers the potential to improve predictions concerning the dispersion of contaminants or solutes within aquifers, accounting for preferential flow pathways and deviations from Fickian behavior. In the realm of hydrocarbon exploration, a comprehensive understanding of nonlocal transport can lead to more accurate prognostications regarding reservoir dynamics

and the intricate flow patterns of fluids within intricate geological structures. Furthermore, within environmental engineering processes, our model has the potential to contribute to the development of more efficient strategies for the transportation and containment of hazardous substances, taking into consideration the non-Fickian diffusion characteristics inherent in such processes.

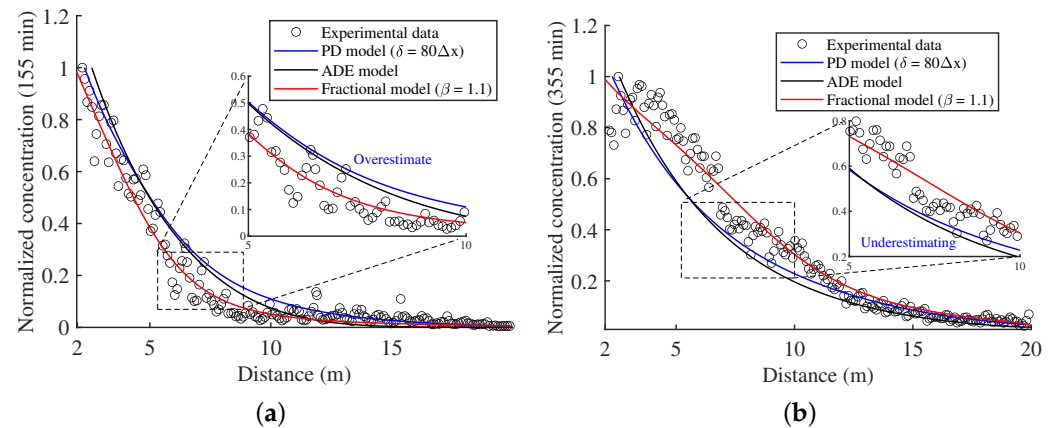


Figure 6. Modeled (lines) versus observed (symbols) snapshots for bedload sediments with a diameter of 1 mm; three models were compared: the classical ADE model (black lines), the PD model (a circular influence domain with radius $\delta = 80\Delta x$) (blue lines), and the fractional Laplacian-based model (fractional order $\beta = 1.1$) (red lines) at two times ($t = 155$ min and 355 min) along the 20 m long flume. (a) $t = 155$ min, (b) $t = 355$ min.

5. Conclusions

This study aimed at refining the classical fractional model to quantify the observed nonlocal diffusion processes in both forward and backward directions during tracer transport within bounded heterogeneous systems. The analysis and application of the fractional Laplacian-based model enhance our understanding of the complex nature of nonlocal tracer transport. Three main conclusion can be drawn from this study:

1. Nonlocal dynamics result in early arrivals of tracer particles and the emergence of heavy-tailed distributions, underscoring the intricate nature of space nonlocal transport processes. The utilization of the fractional Laplacian-based model proved to be highly effective in accurately describing nonlocal tracer transport encompassing both forward and backward diffusion processes;

2. The inherent infinite nonlocal nature of the fractional Laplacian poses significant challenges when it comes to numerically approximating it within finite domains, and tracer nonlocal transport must be incorporated into these characterizations in mathematical ways on bounded domains. The Riesz fractional Laplacian provides a mathematical framework for describing tracer diffusion processes on a bounded domain, and the novel FDM demonstrated its suitability as a good solution for the fractional Laplacian-based model on a bounded domain;

3. The application emphasizes that nonlocal transport processes exhibit dynamic characteristics, influenced by the evolving heterogeneity of the media at various temporal scales. The evolving fractional order parameter, denoted as β , holds significant importance in assessing nonlocal transport behavior. Notably, β displays a decreasing trend over time, signifying an intensification in the nonlocal aspects of tracer transport as time progresses.

Author Contributions: Conceptualization, Z.L.; methodology, Z.L. and H.Z.; formal analysis, Z.L. and L.K.; investigation, H.Z. and L.K.; resources, H.T., S.Y. and H.S.; writing—original draft preparation, Z.L. and H.S.; writing—review and editing, H.T., H.Z., L.K. and H.S.; visualization, Z.L. and L.K.; funding acquisition, Z.L., H.T. and S.Y.; supervision, H.T., S.Y. and H.S. All authors have read and agreed to the published version of the manuscript.

Funding: This work was supported by the National Key R&D Program of China (2022YFC3202602), the project of Key Laboratory of Changjiang Regulation and Protection of Ministry of Water Resources (CX2023K03), the National Natural Science Foundation of China (52309087), the China Postdoctoral Science Foundation (2022M711024), the Jiangsu Funding Program for Excellent Postdoctoral Talent (2022ZB180).

Data Availability Statement: Data are contained within the article.

Conflicts of Interest: The authors declare no conflicts of interest.

References

1. Bouchaud, J.P.; Georges, A. Anomalous diffusion in disordered media: Statistical mechanisms, models and physical applications. *Phys. Rep.* **1990**, *195*, 127–293. [[CrossRef](#)]
2. Berkowitz, B.; Cortis, A.; Dentz, M.; Scher, H. Modeling non-Fickian transport in geological formations as a continuous time random walk. *Rev. Geophys.* **2006**, *44*, RG2003. [[CrossRef](#)]
3. Wang, Y.; Sun, H.; Fan, S.; Gu, Y.; Yu, X. A nonlocal fractional peridynamic diffusion model. *Fractal Fract.* **2021**, *5*, 76. [[CrossRef](#)]
4. Li, Z.; Yuan, S.; Tang, H.; Zhu, Y.; Sun, H. Quantifying nonlocal bedload transport: A regional-based nonlocal model for bedload transport from local to global scales. *Adv. Water Resour.* **2023**, *177*, 104444. [[CrossRef](#)]
5. Hao, X.; Sun, H.; Zhang, Y.; Li, S.; Yu, Z. Co-transport of arsenic and micro/nano-plastics in saturated soil. *Environ. Res.* **2023**, *228*, 115871. [[CrossRef](#)] [[PubMed](#)]
6. Hatano, Y.; Hatano, N. Dispersive transport of ions in column experiments: An explanation of long-tailed profiles. *Water Resour. Res.* **1998**, *34*, 1027–1033. [[CrossRef](#)]
7. Liu, L.; Zhang, S.; Chen, S.; Liu, F.; Feng, L.; Turner, I.; Zheng, L.; Zhu, J. An Application of the Distributed-Order Time-and Space-Fractional Diffusion-Wave Equation for Studying Anomalous Transport in Comb Structures. *Fractal Fract.* **2023**, *7*, 239. [[CrossRef](#)]
8. Li, Z.; Kiani Oshorjani, M.; Chen, D.; Zhang, Y.; Sun, H. Dynamics of Dual-Mode Bedload Transport With Three-Dimensional Alternate Bars Migration in Subcritical Flow: Experiments and Model Analysis. *J. Geophys. Res. Earth Surf.* **2023**, *128*, e2022JF006882. [[CrossRef](#)]
9. Adams, E.E.; Gelhar, L.W. Field study of dispersion in a heterogeneous aquifer: 2. Spatial moments analysis. *Water Resour. Res.* **1992**, *28*, 3293–3307. [[CrossRef](#)]
10. Zhang, Y.; Benson, D.A.; Reeves, D.M. Time and space nonlocalities underlying fractional-derivative models: Distinction and literature review of field applications. *Adv. Water Resour.* **2009**, *32*, 561–581. [[CrossRef](#)]
11. Metzler, R.; Rajyaguru, A.; Berkowitz, B. Modelling anomalous diffusion in semi-infinite disordered systems and porous media. *New J. Phys.* **2022**, *24*, 123004. [[CrossRef](#)]
12. Sun, H.; Zhang, Y.; Baleanu, D.; Chen, W.; Chen, Y. A new collection of real world applications of fractional calculus in science and engineering. *Commun. Nonlinear Sci. Numer. Simul.* **2018**, *64*, 213–231. [[CrossRef](#)]
13. ten Hagen, B.; van Teeffelen, S.; Löwen, H. Brownian motion of a self-propelled particle. *J. Phys. Condens. Matter* **2011**, *23*, 194119. [[CrossRef](#)]
14. Ghosh, P.K.; Misko, V.R.; Marchesoni, F.; Nori, F. Self-propelled Janus particles in a ratchet: Numerical simulations. *Phys. Rev. Lett.* **2013**, *110*, 268301. [[CrossRef](#)] [[PubMed](#)]
15. Nelissen, K.; Misko, V.; Peeters, F. Single-file diffusion of interacting particles in a one-dimensional channel. *Europhys. Lett.* **2007**, *80*, 56004. [[CrossRef](#)]
16. Taloni, A.; Marchesoni, F. Single-file diffusion on a periodic substrate. *Phys. Rev. Lett.* **2006**, *96*, 020601. [[CrossRef](#)]
17. Boffetta, G.; De Lillo, F.; Musacchio, S. Anomalous diffusion in confined turbulent convection. *Phys. Rev. E* **2012**, *85*, 066322. [[CrossRef](#)]
18. Metzler, R.; Klafter, J. The random walk's guide to anomalous diffusion: A fractional dynamics approach. *Phys. Rep.* **2000**, *339*, 1–77. [[CrossRef](#)]
19. Sun, L.; Qiu, H.; Wu, C.; Niu, J.; Hu, B.X. A review of applications of fractional advection–dispersion equations for anomalous solute transport in surface and subsurface water. *Wiley Interdiscip. Rev. Water* **2020**, *7*, e1448. [[CrossRef](#)]
20. Cushman, J.H. *The Physics of Fluids in Hierarchical Porous Media: Angstroms to Miles*; Springer Science & Business Media: Berlin/Heidelberg, Germany, 2013; Volume 10.
21. Fofoula-Georgiou, E.; Ganti, V.; Dietrich, W. A nonlocal theory of sediment transport on hillslopes. *J. Geophys. Res. Earth Surf.* **2010**, *115*, F00A16. [[CrossRef](#)]
22. Union, J.I.G. Advection diffusion equation models in near-surface geophysical and environmental sciences. *J. Indian Geophys. Union* **2013**, *17*, 117–127.
23. Hilfer, R. *Applications of Fractional Calculus in Physics*; World Scientific: Singapore, 2000.
24. Klafter, J.; Lim, S.; Metzler, R. *Fractional Dynamics: Recent Advances*; World Scientific: Singapore, 2012.
25. Tawfik, A.M.; Hefny, M.M. Subdiffusive Reaction Model of Molecular Species in Liquid Layers: Fractional Reaction-Telegraph Approach. *Fractal Fract.* **2021**, *5*, 51. [[CrossRef](#)]

26. Kim, S.; Kavvas, M.L. Generalized Fick's law and fractional ADE for pollution transport in a river: Detailed derivation. *J. Hydrol. Eng.* **2006**, *11*, 80–83. [[CrossRef](#)]
27. Baeumer, B.; Kovács, M.; Meerschaert, M.M.; Sankaranarayanan, H. Reprint of: Boundary conditions for fractional diffusion. *J. Comput. Appl. Math.* **2018**, *339*, 414–430. [[CrossRef](#)]
28. Zhang, Y.; Yu, X.; Li, X.; Kelly, J.F.; Sun, H.; Zheng, C. Impact of absorbing and reflective boundaries on fractional derivative models: Quantification, evaluation and application. *Adv. Water Resour.* **2019**, *128*, 129–144. [[CrossRef](#)]
29. Jannelli, A.; Ruggieri, M.; Speciale, M.P. Analytical and numerical solutions of time and space fractional advection–diffusion–reaction equation. *Commun. Nonlinear Sci. Numer. Simul.* **2019**, *70*, 89–101. [[CrossRef](#)]
30. Yin, M.; Ma, R.; Zhang, Y.; Chen, K.; Guo, Z.; Zheng, C. A Dual Heterogeneous Domain Model for Upscaling Anomalous Transport With Multi-Peaks in Heterogeneous Aquifers. *Water Resour. Res.* **2022**, *58*, e2021WR031128. [[CrossRef](#)]
31. Angstmann, C.N.; Henry, B.I.; Jacobs, B.A.; McGann, A.V. An explicit numerical scheme for solving fractional order compartment models from the master equations of a stochastic process. *Commun. Nonlinear Sci. Numer. Simul.* **2019**, *68*, 188–202. [[CrossRef](#)]
32. Furbish, D.J.; Roering, J.J. Sediment disentrainment and the concept of local versus nonlocal transport on hillslopes. *J. Geophys. Res. Earth Surf.* **2013**, *118*, 937–952. [[CrossRef](#)]
33. Zhang, Y. Backward Particle Tracking of Anomalous Transport in Multi-Dimensional Aquifers. *Water Resour. Res.* **2022**, *58*, e2022WR032396. [[CrossRef](#)]
34. Lischke, A.; Pang, G.; Gulian, M.; Song, F.; Glusa, C.; Zheng, X.; Mao, Z.; Cai, W.; Meerschaert, M.M.; Ainsworth, M.; et al. What is the fractional Laplacian? A comparative review with new results. *J. Comput. Phys.* **2020**, *404*, 109009. [[CrossRef](#)]
35. Scherer, R.; Kalla, S.L.; Tang, Y.; Huang, J. The Grünwald–Letnikov method for fractional differential equations. *Comput. Math. Appl.* **2011**, *62*, 902–917. [[CrossRef](#)]
36. Li, C.; Qian, D.; Chen, Y. On Riemann–Liouville and Caputo derivatives. *Discret Dyn. Nat. Soc.* **2011**, *2011*, 562494. [[CrossRef](#)]
37. De Oliveira, E.C.; Tenreiro Machado, J.A. A review of definitions for fractional derivatives and integral. *Math. Probl. Eng.* **2014**, *2014*, 238459. [[CrossRef](#)]
38. Zoia, A.; Rosso, A.; Kardar, M. Fractional Laplacian in bounded domains. *Phys. Rev. E* **2007**, *76*, 021116. [[CrossRef](#)]
39. D'Elia, M.; Gunzburger, M. The fractional Laplacian operator on bounded domains as a special case of the nonlocal diffusion operator. *Comput. Math. Appl.* **2013**, *66*, 1245–1260. [[CrossRef](#)]
40. Zhang, Y.; Zhou, D.; Yin, M.; Sun, H.; Wei, W.; Li, S.; Zheng, C. Nonlocal transport models for capturing solute transport in one-dimensional sand columns: Model review, applicability, limitations and improvement. *Hydrol. Process.* **2020**, *34*, 5104–5122. [[CrossRef](#)]
41. Duo, S.; van Wyk, H.W.; Zhang, Y. A novel and accurate finite difference method for the fractional Laplacian and the fractional Poisson problem. *J. Comput. Phys.* **2018**, *355*, 233–252. [[CrossRef](#)]
42. Gao, T.; Duan, J.; Li, X.; Song, R. Mean exit time and escape probability for dynamical systems driven by Lévy noises. *SIAM J. Sci. Comput.* **2014**, *36*, A887–A906. [[CrossRef](#)]
43. Huang, Y.; Oberman, A. Numerical methods for the fractional Laplacian: A finite difference–quadrature approach. *SIAM J. Numer. Anal.* **2014**, *52*, 3056–3084. [[CrossRef](#)]
44. Sun, H.; Li, Z.; Zhang, Y.; Chen, W. Fractional and fractal derivative models for transient anomalous diffusion: Model comparison. *Chaos Solitons Fractals* **2017**, *102*, 346–353. [[CrossRef](#)]
45. Yin, M.; Zhang, Y.; Ma, R.; Tick, G.R.; Bianchi, M.; Zheng, C.; Wei, W.; Wei, S.; Liu, X. Super-diffusion affected by hydrofacies mean length and source geometry in alluvial settings. *J. Hydrol.* **2020**, *582*, 124515. [[CrossRef](#)]

Disclaimer/Publisher's Note: The statements, opinions and data contained in all publications are solely those of the individual author(s) and contributor(s) and not of MDPI and/or the editor(s). MDPI and/or the editor(s) disclaim responsibility for any injury to people or property resulting from any ideas, methods, instructions or products referred to in the content.